

# A DFT Analysis of the Molecular Structures and Vibrational Spectra of Diphenylsulfone and 4,4'-Sulfonyldianiline (Dapsone)

Wolfgang Förner and Hassan M. Badawi

Department of Chemistry, King Fahd University of Petroleum & Minerals, Dhahran 31261, Saudi Arabia

Reprint requests to W. Förner. Fax: 966 3 8605503. E-mail: forner@kfupm.edu.sa

*Z. Naturforsch.* **2011**, *66b*, 69–76; received October 11, 2010

We have performed density functional calculations with the B3LYP functional and a 6-311G\*\* basis set to obtain the vibrational spectra in harmonic approximation of the anti-leprosy drug Dapsone and the parent compound diphenylsulfone. Although the chemical difference between the two molecules is not that pronounced (Dapsone has amino groups in the *para* positions in the phenyl rings), Dapsone is an active drug, while to our knowledge diphenylsulfone shows no medical activity. We compared the theoretical results to experimental vibrational spectra found in the literature. With the help of the program GAUSSVIEW we were able to assign the experimentally found spectral lines to specific atomic motions. The remarkable difference between the two molecules, regarding their structural behavior, is that the drug Dapsone has a more flexible structure of the phenyl ring than the parent molecule has. This might contribute to a greater ability of the drug to fit into receptor sites in a cell membrane although one has to be well aware that this plays most probably only a minor role in the drug activity of Dapsone.

**Key words:** Conformational Behavior, Vibrational Spectra and Assignments, Diphenylsulfone, 4,4'-Sulfonyldianiline, Dapsone

## Introduction

The interesting structure of aniline was the subject of many theoretical and experimental studies, and the pyramidal conformation of its nitrogen atom is well established in the literature [1–5]. The non-planarity was reported to be a result of a balance between two opposing forces: the *p-p* conjugation of the nitrogen lone pair with the aromatic ring and the energy gained from highly directed *sp*<sup>3</sup> orbitals for the C–N bond formation [1]. A symmetric near-planar structure with *C*<sub>s</sub> molecular symmetry and an HNCC torsional angle (angle between the NH and the CC bonds as viewed along the NC bond) of about 20 degrees was predicted on DFT-B3LYP, MP2, MP4(SDTQ) and CCSD(T) levels of calculations with a 6-311G\*\* basis set to be a real minimum on the potential surface of aniline [5]. At this low-energy form, the two N–H bonds are directed symmetrically towards the same side of the benzene ring. The NH<sub>2</sub> inversion barrier was predicted at the MP2 level of theory to be 2.1 kcal mol<sup>–1</sup> [5].

On the other side of the N atom the lone pair has the right direction to overlap with the  $\pi^*$  orbitals of the ring. In this way the aromaticity of the phenyl

group is not much reduced, and the electrons donated from the -NH<sub>2</sub> group into the antibonding  $\pi^*$  system stabilize the molecule due to this negative hyperconjugation effect. Such a negative hyperconjugation has been described by Wojciechowski *et al.* [1] in their analysis of the natural bond orbital interactions in aniline. Further it is indicated by the slight lowering of the pyramidalization of the -NH<sub>2</sub> group. Note that the above arguments hold also when the benzene ring H atoms next to the -NH<sub>2</sub> group are substituted by Cl atoms [5].

The *planar* structure of aniline was reported to be a clear transition state, since in a *planar* -NH<sub>2</sub> group the lone pair at nitrogen would be of purely 2*p<sub>z</sub>* character, and thus it would be involved in conjugation with the phenyl ring. Such a conjugation would certainly stabilize the *planar* -NH<sub>2</sub> group, but would destabilize the molecule as a whole, since conjugation would drastically reduce the aromatic character of the phenyl ring as for example in the aniline radical cation where, due to conjugation, the phenyl ring has an almost quinoidal character [1]. Thus the *planar* form (with a planar NH<sub>2</sub> group) was reported to be a transition state of the -NH<sub>2</sub> inversion [5].

As a continuation of the investigations of the properties of substituted anilines we investigated the conformational stability and analyzed the vibrational spectra of the important sulfa drug Dapsone (4,4'-sulfonyldianiline) in the present study. The work was extended to diphenylsulfone as the main building block of Dapsone for the purpose of comparison. Further we were interested in the question whether or not there are clear differences in the vibrational behavior of the two molecules which might be a minor part of the reason why one of them (Dapsone) is a drug, while the other one (diphenylsulfone) to our knowledge shows no such medical activity. The reason is probably not an electronic one, since as outlined below the structure does not allow a back donation of electron density from the oxygen lone pairs into the antibonding part of the aromatic system. However, as discussed already for aniline, the lone pair on the nitrogen atoms should make the rings more electron rich than those in diphenylsulfone, which might well contribute to the medical activity of Dapsone. Density Functional B3LYP and *ab initio* MP2 calculations were employed in the study. The 6-311G\*\* basis set was utilized in these calculations. The energies of the compounds in their stable conformations and the transition states were optimized at the two levels of calculation. The vibrational frequencies of both molecules in their ground-state structure were calculated at DFT-B3LYP level. The calculated wavenumbers are compared to experimental results. Complete vibrational assignments of the calculated normal modes were made on the basis of the results of GAUSSVIEW visualizations of calculated normal modes and experimental data, since it is of importance to have a clear knowledge, to what motions of atoms an observed vibrational line belongs and what might be the reason if during a modification a line would become diminished or enhanced.

### Computational Details and Minimum Structures

The GAUSSIAN 03 program [6], running on a 128 node High-performance e-1350 IBM Cluster, was used to carry out the DFT-B3LYP and the MP2 calculations. The 6-311G\*\* basis set was employed to optimize the structures and predict the energies and the dipole moments of diphenylsulfone and 4,4'-sulfonyldianiline in their possible structures (Fig. 1). The optimized structural parameters (on DFT level only) and energies of the molecules at the DFT-B3LYP and MP2 levels are listed in Tables 1 and 2, while the calculated mini-

Table 1. Calculated (DFT) and experimental structural parameters for diphenylsulfone (X denotes H) and 4,4'-sulfonyldianiline (X denotes N), rotational constants and dipole moments (see Fig. 1 for atom numbering).

	Diphenylsulfone		4,4'-Sulfonyldianiline	
	calculated	experimental [7]	calculated	experimental [8]
Bond lengths (Å)				
S <sub>1</sub> O <sub>4</sub>	1.47	1.449	1.47	1.45
S <sub>1</sub> C <sub>3</sub>	1.81	1.764	1.79	1.76
C <sub>3</sub> C <sub>11</sub>	1.39		1.39	1.37
C <sub>11</sub> C <sub>13</sub>	1.39		1.39	1.40
C <sub>13</sub> C <sub>15</sub>	1.39		1.41	1.38
C <sub>15</sub> X <sub>25</sub>	1.08		1.38	1.39
N <sub>25</sub> H <sub>29</sub>	–		1.01	1.0
C <sub>11</sub> H <sub>21</sub>	1.08		1.08	1.1
C <sub>13</sub> H <sub>23</sub>	1.08		1.09	1.0
Bond angles (deg)				
O <sub>4</sub> S <sub>1</sub> C <sub>3</sub>	107.4	108.6	107.2	108.1
S <sub>1</sub> C <sub>3</sub> C <sub>11</sub>	119.2		119.9	117.8
C <sub>3</sub> C <sub>11</sub> C <sub>13</sub>	118.9		119.9	117.8
C <sub>11</sub> C <sub>13</sub> C <sub>15</sub>	120.1		120.7	119.8
C <sub>13</sub> C <sub>15</sub> C <sub>14</sub>	120.3		118.6	121.9
C <sub>13</sub> C <sub>15</sub> X <sub>25</sub>	119.8		120.7	117.0
C <sub>15</sub> N <sub>25</sub> H <sub>29</sub>	–		116.6	127
C <sub>3</sub> C <sub>11</sub> H <sub>21</sub>	119.9		119.7	122
C <sub>11</sub> C <sub>13</sub> H <sub>23</sub>	119.7		119.8	120
Dihedral angles (deg)				
O <sub>4</sub> S <sub>1</sub> C <sub>3</sub> C <sub>11</sub>	23.3	28.1	23.7	
C <sub>13</sub> C <sub>15</sub> N <sub>25</sub> H <sub>29</sub>	–		–22.1	
C <sub>11</sub> C <sub>13</sub> C <sub>15</sub> X <sub>25</sub>	–179.9		–177.3	
C <sub>3</sub> S <sub>1</sub> C <sub>2</sub> C <sub>6</sub>	90.4	86.6	90.2	
Rotational constants (GHz)				
A	0.9262		0.7233	
B	0.3810		0.2483	
C	0.3583		0.2228	
Dipole moments (D)				
$\mu$	5.65		6.57	

um structure and atom numbering of Dapsone (in diphenylsulfone the N<sub>20</sub>H<sub>26</sub>H<sub>27</sub> group is replaced by H<sub>20</sub> and the N<sub>25</sub>H<sub>28</sub>H<sub>29</sub> group by H<sub>25</sub>, while the structures of the diphenylsulfone parts are rather similar in both molecules) is shown in Fig. 1. As is obvious from Table 1, the few comparable X-ray structure data from ref. [7] for diphenylsulfone agree rather well with our calculated ones, given that solid-state effects are absent in our calculations. Further, as is also obvious from Table 1, we conclude that DFT together with our basis set yields a very reliable structure also for Dapsone as compared with the X-ray data [8]. Actually, the most noticeable discrepancies regard the H atom positions which are ill-defined in the experimental structure determination (film data). The poor data set used for the crystal structure determination might also be responsible for differences in bond lengths and angles observed in the phenyl rings [8].

Table 2. Calculated total energies  $E$  (in Hartrees) of possible structures together with energy differences  $\Delta E$  (kcal mol<sup>-1</sup>) to the corresponding lowest-energy structures of diphenylsulfone and Dapsone at DFT-B3LYP and MP2 (both using a 6-311G\*\* basis set) levels of theory<sup>a</sup>.

Structure	( $\phi_1, \phi_2$ ) <sup>a</sup>	$E$ (H)	$\Delta E$ (kcal mol <sup>-1</sup> )
Diphenylsulfone (DFT-B3LYP)			
perpendicular	(90°, -)	-1012.047919	0.00
co-planar	(0°, -)	-1012.009099	24.36
Diphenylsulfone (MP2)			
perpendicular	(90°, -)	-1009.739657	0.00
co-planar	(0°, -)	-1009.694498	28.34
Dapsone (DFT-B3LYP)			
perpendicular	(90°, 21°)	-1122.799697	0.00
NH <sub>2</sub> inversion TS <sup>a</sup>	(90°, 0°)	-1122.798046	1.04
co-planar (TS <sup>a</sup> )	(0°, 0°)	-1122.756879	26.87
Dapsone (MP2)			
perpendicular	(90°, 26°)	-1120.197216	0.00
NH <sub>2</sub> inversion TS <sup>a</sup>	(90°, 0°)	-1120.191453	3.62
co-planar (TS <sup>a</sup> )	(0°, 0°)	-1120.144670	32.97

<sup>a</sup>  $\phi_1$  denotes the torsional angle CCSO and  $\phi_2$  the torsional angle HNCC; “perpendicular” denotes the conformer with  $\phi_1 = 90^\circ$ , “co-planar” that with  $\phi_1 = 0^\circ$ ; TS stands for the planar transition state of the NH<sub>2</sub> inversion.

Although only DFT structural parameters are listed in Table 1, in the absolute minimum structures of both molecules there is not much a difference between DFT and MP2 results. The OSC bond angle of about 107° is reasonably close to the expected tetrahedral angle at the sulfur atom. The absolute minimum is termed perpendicular, because the CSCC dihedral angle (being the angle between the C<sub>3</sub>S<sub>1</sub> and the C<sub>2</sub>C<sub>6</sub> bonds, projected onto a plane perpendicular to the S<sub>1</sub>C<sub>2</sub> bond, or – both are equal – the angle between the C<sub>2</sub>S<sub>1</sub> and the C<sub>3</sub>C<sub>12</sub> bonds, projected onto a plane perpendicular to the S<sub>1</sub>C<sub>3</sub> bond) in both structures is almost 90°. Thus the planes of the phenyl rings in the minimum face each other in an almost C<sub>2v</sub> symmetry. As explained in the Introduction, the situation at the -NH<sub>2</sub> groups in Dapsone is – as expected – very similar to the corresponding one in our previously published results on chlorine-substituted anilines [5], with a pyramidal -NH<sub>2</sub> group having both hydrogens on the same side of the corresponding phenyl ring.

Since the S(3d)O(2p)  $\pi$  bonds are in the same plane as the SO<sub>2</sub> group, the lone pairs on the oxygen atoms are perpendicular to the plane, and thus point into the space above a phenyl ring, but are situated quite far away from the ring plane. Thus, although one cannot exclude that some back-donation of electrons between lone pairs and the antibonding ring  $\pi^*$  orbitals might occur (negative hyperconjugation), we expect its effect

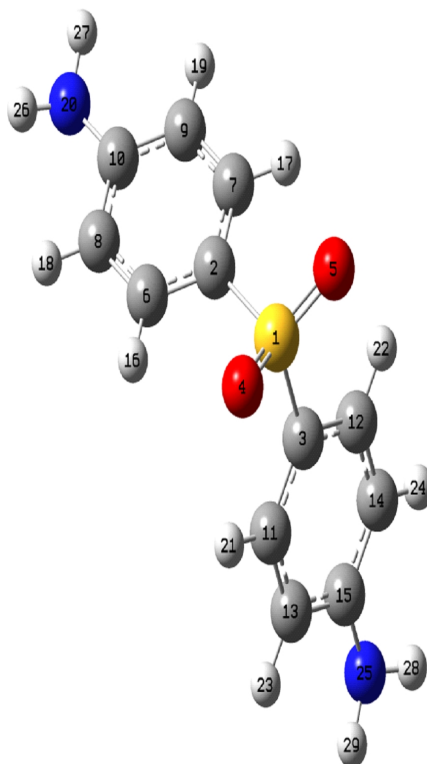


Fig. 1. Atom numbering and DFT-optimized structure for Dapsone (in case of diphenylsulfone N<sub>20</sub>H<sub>26</sub>H<sub>27</sub> are replaced by H<sub>20</sub> and N<sub>25</sub>H<sub>28</sub>H<sub>29</sub> are replaced by H<sub>25</sub>).

on the structure of the system, if present at all, not to be too large.

In Table 1 we include for comparison a few experimental data we found in the literature for diphenylsulfone, and it is obvious that these agree reasonably well with our calculated ones. The structural data given in the table were calculated using DFT with a B3LYP (Becke-3-Lee-Yang-Parr) potential and a valence triple zeta basis augmented by polarization functions (6-311G\*\*). From the X-ray data for Dapsone in reference [8] there is fair agreement between our calculated and the experimental structural data. What regards the phenyl rings, in a previous paper we compared calculated structures (with a somewhat smaller valence double zeta basis set, 6-31G\*\*) [9] with experimental data for biphenyl, again finding reasonable agreement. Thus one can conclude that our computational method should be well applicable to Dapsone and diphenylsulfone. Also the reasonable agreement between calculated and experimental wavenumbers (as detailed in Tables 3 and 4) for the two systems makes us confident that our data can be trusted.

Table 3. Calculated (dp denotes calculated depolarization ratio) and observed wavenumbers (Infrared and Raman spectra) [21, 22] together with the ratio of observed to calculated wavenumbers (always with the observed infrared wavenumbers if possible) and the assignment of the vibrations to atomic motions based on the program GAUSSVIEW for diphenylsulfone ( $C_{2v}$ :  $20 A_1 + 15 A_2 + 20 B_1 + 14 B_2 = 69$  modes) where def. stands for deformation, (+) or (–) indicates that the corresponding motions in one ring are added or subtracted from those in the other ring, s denotes symmetric, as antisymmetric.

Symm.	calcd. (dp)	— Wavenumber (cm <sup>-1</sup> ) —		obs./calcd.	Assignment
		Infrared <sup>a</sup>	Raman <sup>a</sup>		
B <sub>2</sub>	117 (0.75)		111 (w)	0.95	SO <sub>2</sub> rock + ring def. (–)
A <sub>2</sub>	199 (0.75)		185 (vw)	0.93	SO <sub>2</sub> scissor + ring def. (–)
A <sub>1</sub>	241 (0.60)		249 (w)	1.03	CSC bend + ring def. (–)
B <sub>2</sub>	296 (0.75)		302 (w)	1.02	CS as stretch
A <sub>1</sub>	305 (0.11)		313 (w)	1.03	CS s stretch
A <sub>2</sub>	324 (0.75)		334 (vw, shd)	1.03	SO <sub>2</sub> scissor – ring def. (+)
B <sub>1</sub>	453 (0.75)		462 (vw)	1.02	S – ring in plane bend
A <sub>1</sub>	558 (0.31)	559 (vs)	568 (vw)	1.00	SO <sub>2</sub> bend + ring def. (+)
B <sub>2</sub>	594 (0.75)	585 (vs)		0.98	$\alpha$ CH <sub>2</sub> + $\beta$ CH <sub>2</sub> s wag (–)
A <sub>2</sub>	628 (0.75)	601 (vw)	611 (vw)	0.96	in plane as ring def. (–)
B <sub>2</sub>	700 (0.75)	681 (s)		0.97	$\alpha$ CH <sub>2</sub> + $\gamma$ CH s wag (–)
B <sub>2</sub>	730 (0.75)	734 (vs)		1.01	in plane s ring def. (–)
B <sub>2</sub>	764 (0.75)	766 (s)		1.00	CS as stretch
B <sub>2</sub>	937 (0.75)	936 (vw)		1.00	$\alpha$ CH <sub>2</sub> – $\beta$ CH <sub>2</sub> – $\gamma$ CH s wag (–)
A <sub>1</sub>	1013 (0.01)	1000 (m)	994 (vs)	0.99	as in plane ring def. (–)
B <sub>2</sub>	1015 (0.75)		1015 (w)	1.00	as in plane ring def. (–)
A <sub>1</sub>	1039 (0.07)	1032 (vw)		0.99	ring breathing (+)
A <sub>1</sub>	1064 (0.72)	1064 (w)	1068 (vw)	1.00	$\alpha$ CH <sub>2</sub> – $\beta$ CH <sub>2</sub> s in plane bend (+)
B <sub>2</sub>	1098 (0.75)	1106 (s)		1.01	$\alpha$ CH <sub>2</sub> – $\beta$ CH <sub>2</sub> s in plane bend (–)
B <sub>1</sub>	1101 (0.75)		1143 (m)	1.04	$\alpha$ CH <sub>2</sub> – $\beta$ CH <sub>2</sub> as + $\gamma$ CH in plane bend (+)
A <sub>1</sub>	1126 (0.03)	1160 (vs)		1.03	SO s stretch
B <sub>1</sub>	1185 (0.75)	1186 (w)	1185 (vw)	1.00	$\alpha$ CH <sub>2</sub> – $\beta$ CH <sub>2</sub> as – $\gamma$ CH in plane bend (+)
B <sub>1</sub>	1288 (0.75)	1293 (s)	1291 (s)	1.00	SO as stretch
B <sub>1</sub>	1332 (0.75)	1314 (vs)		0.99	ring in plane as def. (+)
B <sub>1</sub>	1347 (0.75)	1324 (s)		0.98	ring in plane as def. (+)
B <sub>1</sub>	1479 (0.75)	1447 (s)		0.98	ring in plane as def. (+)
B <sub>2</sub>	1506 (0.75)	1479 (vw)		0.98	ring in plane as def. (–)
A <sub>2</sub>	1625 (0.75)		1568 (m)	0.96	SC <sub>2</sub> scissor + ring def. (–)
A <sub>1</sub>	1625 (0.49)	1585 (vw)		0.98	ring in plane s def. (+)
B <sub>1</sub>	1630 (0.75)	1617 (vw)		0.99	ring in plane s def. (+)
B <sub>2</sub>	3170 (0.75)	2979 (vw)	2983 (vw, shd)	0.94	$\alpha$ CH <sub>2</sub> – $\beta$ CH <sub>2</sub> s + $\gamma$ CH stretch (–)
A <sub>1</sub>	3170 (0.71)	3000(vw)		0.95	$\alpha$ CH <sub>2</sub> – $\beta$ CH <sub>2</sub> s + $\gamma$ CH stretch (+)
A <sub>2</sub>	3181 (0.75)		3047(s)	0.96	$\alpha$ CH <sub>2</sub> – $\beta$ CH <sub>2</sub> as stretch (–)
B <sub>1</sub>	3181 (0.75)	3064(vw)	3057(w)	0.96	$\alpha$ CH <sub>2</sub> – $\beta$ CH <sub>2</sub> as stretch (+)
B <sub>2</sub>	3191 (0.75)	3096(vw)		0.97	$\alpha$ CH <sub>2</sub> – $\beta$ CH <sub>2</sub> s – $\gamma$ CH stretch (–)

<sup>a</sup> Intensities: v = very, w = weak, m = medium, s = strong, shd = shoulder. From measured peak heights these are:  $0 < vw < 20\%$ ,  $20 < w < 40\%$ ,  $40 < m < 60\%$ ,  $60 < s < 80\%$ ,  $80 < vs < 100\%$ , percentage of peak height of the strongest line.

In our opinion the large energy differences between co-planar (phenyl planes parallel to the SO<sub>2</sub> plane) and perpendicular (phenyl planes perpendicular to the SO<sub>2</sub> plane) geometries should be mostly due to steric effects (see Table 2 for a definition of these geometries). Any rotation of a phenyl ring out of the perpendicular arrangement would lead to the hydrogens of the rotated ring pointing to the other ring plane with rather close distances. Thus even the rotation of only one ring out of the perpendicular arrangement should increase the energy of the structure. This effect becomes far more dramatic in the co-planar structure, where the hydrogens of the two rings are at close distance and thus

in a highly repulsive geometry, indicated by the large energy differences between planar and perpendicular structures. The differences between DFT and MP2 relative energies have their reason in our case in the fact that we are dealing with non-bonding interactions, and it is well known that DFT is not too accurate in the calculation of energy differences due to such effects.

### Vibrational Wavenumbers, Spectra and Assignments of Normal Modes

The optimized structural parameters of diphenylsulfone and 4,4'-sulfonyldianiline were used to calculate

Table 4. Calculated (dp denotes calculated depolarization ratio) and observed wavenumbers (Infrared and Raman spectra) [17] together with the ratio of observed to calculated wavenumbers (always with the observed infrared wavenumbers if possible) and the assignment of the vibrations to atomic motions based on the program GAUSSVIEW for 4,4'-sulfonyldianiline (Dapsone,  $C_{2v}$ :  $23 A_1 + 18 A_2 + 20 B_1 + 20 B_2 = 81$  modes) where def. stands for deformation, (+) or (–) indicates that the corresponding motions in one ring are added or subtracted from those in the other ring, s denotes symmetric, as antisymmetric.

Symm.	calcd. (dp)	— Wavenumber (cm <sup>-1</sup> ) —		obs./calcd.	Assignment
		Infrared <sup>a</sup>	Raman <sup>a</sup>		
A <sub>1</sub>	32 (0.72)		32 (ms)	1.00	CSC bend
B <sub>2</sub>	107 (0.75)		107 (m)	1.00	SO <sub>2</sub> rock + ring def. (–)
A <sub>1</sub>	168 (0.39)	178 (ms)		1.06	CSC bend + ring def. (–)
A <sub>2</sub>	179 (0.75)		184 (w)	1.03	SO <sub>2</sub> scissor + ring def. (–)
B <sub>2</sub>	258 (0.75)		276 (w)	1.07	SO <sub>2</sub> rock + ring def. (+)
B <sub>2</sub>	299 (0.75)		296 (m)	0.99	CC as stretch
B <sub>1</sub>	335 (0.75)		335 (vw)	1.00	NH <sub>2</sub> torsion (+)
B <sub>1</sub>	370 (0.75)	383 (w)	390 (vw)	1.05	NH <sub>2</sub> torsion + ring def. (+)
A <sub>2</sub>	409 (0.75)	410		1.00	NH <sub>2</sub> – ring in plane bend (–)
A <sub>2</sub>	417 (0.75)	420 (vw)		1.01	ring twisting (–)
B <sub>1</sub>	420 (0.75)		424 (w)	1.01	ring twisting (+)
B <sub>1</sub>	472 (0.75)		500 (w)	1.06	CSC rock + in plane ring def. (+)
A <sub>1</sub>	491 (0.11)	510 (vw)	514 (w)	1.04	SO <sub>2</sub> bend + ring def. (+)
A <sub>1</sub>	508 (0.69)	545 (vs)		1.07	CS wag + NH <sub>2</sub> wag (+)
B <sub>2</sub>	521 (0.75)	555 (s, shd)		1.07	CS wag + NH <sub>2</sub> wag (–)
A <sub>1</sub>	554 (0.34)		577 (w)	1.04	SO <sub>2</sub> bend – ring def. (+)
A <sub>1</sub>	640 (0.55)	633 (w)	637 (ms)	0.99	CS s stretch
A <sub>2</sub>	647 (0.75)	648 (w)	654 (w)	1.00	SC <sub>2</sub> scissor + in plane ring def. (–)
B <sub>2</sub>	685 (0.75)	696 (vs)	701 (m)	1.02	CS as stretch + ring def. (–)
B <sub>2</sub>	719 (0.75)	727 (vs)		1.01	CS wag – NH <sub>2</sub> wag (–)
A <sub>1</sub>	829 (0.08)	825 (s)	819 (s, shd)	1.00	ring breathing (–)
A <sub>1</sub>	843 (0.03)		839 (vs)	1.00	ring breathing (+)
B <sub>2</sub>	949 (0.75)	950 (w)		1.00	$\alpha$ CH <sub>2</sub> – $\beta$ CH <sub>2</sub> s wag (–)
A <sub>1</sub>	956 (0.43)	960 (w)		1.00	$\alpha$ CH <sub>2</sub> – $\beta$ CH <sub>2</sub> s wag (+)
B <sub>1</sub>	970 (0.75)	969 (w)	970 (vw)	1.00	$\alpha$ CH <sub>2</sub> – $\beta$ CH <sub>2</sub> as wag (+)
A <sub>1</sub>	1017 (0.43)	1009 (m)	1008 (w)	0.99	in plane ring def. (+)
A <sub>1</sub>	1062 (0.47)	1071 (vs)	1073 (vs)	1.01	SO s stretch + ring breathing (+)
A <sub>1</sub>	1124 (0.10)	1103 (vs)	1107 (vs)	0.98	SO s stretch – ring breathing (+)
B <sub>1</sub>	1151 (0.75)	1146 (vs)	1141 (vvs)	0.99	ring def. (+)
B <sub>1</sub>	1278 (0.75)	1278 (vs)	1282 (w)	1.00	SO as stretch
A <sub>2</sub>	1322 (0.75)	1291 (m, shd)		0.98	$\alpha$ CH <sub>2</sub> – $\beta$ CH <sub>2</sub> as bend (–)
A <sub>1</sub>	1323 (0.08)	1336 (w)		1.01	$\alpha$ CH <sub>2</sub> – $\beta$ CH <sub>2</sub> s bend (+)
B <sub>1</sub>	1362 (0.75)	1430 (m)	1440 (vw)	1.05	in plane ring def. (+)
B <sub>1</sub>	1465 (0.75)	1496 (m)	1500 (ms)	1.02	in plane as (C–C bonds in opposite edges of the ring stretch differently) ring def. (–)
B <sub>2</sub>	1529 (0.75)	1585 (s)		1.04	in plane as ring def. (–)
A <sub>1</sub>	1530 (0.51)		1598 (vvs)	1.04	in plane as ring def. (–)
B <sub>2</sub>	1639 (0.75)	1626 (s)		0.99	in plane s (C–C bonds in opposite edges of the ring stretch in the same way) ring def. (–)
A <sub>1</sub>	1640 (0.35)		1635 (m)	1.00	in plane s ring def. (+)
B <sub>1</sub>	3162 (0.75)	3045 (w)	3044	0.96	$\beta$ CH <sub>2</sub> as stretch (+)
B <sub>2</sub>	3163 (0.75)	3050 (w)	3059	0.96	$\alpha$ CH <sub>2</sub> – $\beta$ CH <sub>2</sub> s stretch (–)
A <sub>1</sub>	3163 (0.11)		3073 (m)	0.97	$\alpha$ CH <sub>2</sub> – $\beta$ CH <sub>2</sub> s stretch (+)
A <sub>1</sub>	3577 (0.12)	3445 (m)		0.96	NH <sub>2</sub> s stretch (+)
A <sub>2</sub>	3678 (0.75)		3464 (w)	0.94	NH <sub>2</sub> as stretch (–)

<sup>a</sup> Intensities: v: very, w: weak, m: medium, s: strong, ms: medium to strong, shd: shoulder.

the vibrational frequencies of the ground state structures at the DFT-B3LYP/6-311G\*\* level of calculation, since it is well known that DFT yields wavenumbers in rather good agreement with experiment. Assignments of the normal modes were carried out using

the program GAUSSVIEW 3.0 for the stable conformers of the molecules instead of normal mode calculations as described previously [10, 11, 23]. The reason for the use of GAUSSVIEW is the presence of some vibrations containing out-of-plane movements of the

phenyl rings which lead to the fact that our set of internal coordinates for phenyl groups is incomplete, lacking ring carbon wagging coordinates needed to describe out-of-plane motions of a phenyl ring.

## Discussion

The interesting properties and medicinal importance of 4,4'-sulfonyldianiline (Dapsone) as a sulfa drug [12–17] have turned our interest to investigate its structural stability in the present study. We extended the work to diphenylsulfone [18, 19] as the main building unit of the sulfa drug to understand the nature of the forces that control the conformational stability of such an important system. In an early study the characteristic vibrational modes of the  $\text{-NH}_2$  and  $\text{SO}_2$  groups and the aromatic ring have been assigned from isotopic shifts and studies in different solvents [17]. The determination of the molecular structure of Dapsone has shown that in the solid state it has a structure that slightly deviates from  $C_{2v}$  symmetry, with the benzene rings almost parallel to each other and both nearly perpendicular to the OSO plane [8] (see Table 2 for a definition of these geometries).

The vibrational modes of Dapsone were correlated by assuming  $C_{2v}$  symmetry of the molecule. In the present study we attempted to provide a more comprehensive structural and vibrational study of Dapsone by combining both theoretical and experimental data.

Diphenylsulfone and 4,4'-sulfonyldianiline in their perpendicular structure have  $C_{2v}$  symmetry. The 69 vibrational modes of diphenylsulfone span the irreducible representations  $20 A_1 + 15 A_2 + 20 B_1 + 14 B_2$  in  $C_{2v}$ , while for 4,4'-sulfonyldianiline the 81 vibrational modes span the irreducible representations  $23 A_1 + 18 A_2 + 20 B_1 + 20 B_2$  in the same group. The following discussion is focused only on the assignments of the intense spectral lines that characterize both molecules (see Tables 3 and 4 for experimental Raman spectra in the solid state as provided by Sigma Aldrich). The IR band positions and Raman line wavenumbers for diphenylsulfone were measured out in the spectra from the links: <http://www.aist.go.jp/RIODB/SDBS> NO. 1420 for the Infrared spectrum [21] and from [sigmaaldrich.com](http://sigmaaldrich.com) for the Raman spectrum (both in the solid state or solution) [22]. The experimental information in Table 4 for Dapsone was taken from ref. [17]. Note, that the agreement in measured and calculated wavenumbers

cannot be too good, because the molecules in the calculations are in the gas phase, while the experimental spectra were recorded in condensed phase leading to intermolecular interactions not present in the calculated models.

There appears an  $A_1$  mode around  $560 \text{ cm}^{-1}$  which is very strong in the Infrared but very weak in the Raman spectrum and can be assigned to  $\text{SO}_2$  bend coupled with a ring deformation. The line (only in the Infrared spectrum) at about  $590 \text{ cm}^{-1}$  is again very strong and could be identified as the theoretical  $\alpha\text{-CH}_2 + \beta\text{-CH}_2$  symmetric wag. The next strong band in the infrared around  $690 \text{ cm}^{-1}$  is  $\alpha\text{-CH}_2 + \gamma\text{-CH}_2$  symmetric wag. At around  $730 \text{ cm}^{-1}$  there follows a band which is very strong in the infrared and corresponds to a symmetric in plane ring deformation. Also, as expected, the  $\text{SC}_2$  antisymmetric stretch is strong in the infrared at around  $765 \text{ cm}^{-1}$ . CH in-plane bends are a strong feature again in the infrared around  $1100 \text{ cm}^{-1}$ , while at  $1160 \text{ cm}^{-1}$  a very strong band appears which is  $\text{SO}_2$  symmetric stretch, while the antisymmetric one is strong both in the Infrared and the Raman spectra around  $1192 \text{ cm}^{-1}$ . Up to about  $1500 \text{ cm}^{-1}$  three strong to very strong features appear in the Infrared, but not in the Raman spectrum, which are all in plane antisymmetric ring deformations. The rest of the features in the spectra are all very weak to medium, while  $\alpha\text{-CH}_2 - \beta\text{-CH}_2$  antisymmetric stretch at  $3047 \text{ cm}^{-1}$  is strong in the Raman spectrum. All other lines are very weak. The obs./calc. ratios (when possible based on observed infrared bands) are between 0.93 and 1.04 as to be expected, besides the lowest wavenumber (experimental) line at  $111 \text{ cm}^{-1}$  with 0.76. However, such low wavenumber features are usually plagued by anharmonicities which are not corrected for in our calculations.

In the case of Dapsone there are many similar features, however, with contributions from the  $\text{-NH}_2$  groups in *para* positions. The experimental line positions are taken from ref. [20]. However, the assignments there, based just on similarities with other molecules, seem to be questionable to us, especially the assignment of the  $107 \text{ cm}^{-1}$  line in the Raman spectrum as a lattice mode, when the sample is in Nujol, *i. e.* without any crystal lattice, while we assign it to  $\text{SO}_2$  rock with ring deformation, just as the  $111 \text{ cm}^{-1}$  line in diphenylsulfone, which we trust more, especially as the  $\text{SO}_2$  scissor with ring deformation appears at practically the same wavenumber ( $184$  and  $185 \text{ cm}^{-1}$ ) in both molecules – which

in [20] is assigned as torsional mode. The torsions are not observed because according to our calculations they appear at extremely low wavenumbers around  $10\text{ cm}^{-1}$ .

The strong vibrations with major  $\text{NH}_2$  contributions in Dapsone are  $\text{NH}_2$  wagging modes together with  $\text{SC}_2$  wagging, which are very strong infrared features at  $545$  and at  $555\text{ cm}^{-1}$ , the latter one being a strong shoulder. Another very strong infrared band is also  $\text{NH}_2$  wagging together with  $\text{SC}_2$  wagging at  $727\text{ cm}^{-1}$ . Finally, at  $3445\text{ cm}^{-1}$  in the Infrared (medium intensity) and at  $3464\text{ cm}^{-1}$  (weak intensity) in the Raman spectrum the  $\text{NH}_2$  symmetric and antisymmetric stretches are observed. Regarding normal modes which do not include  $\text{NH}_2$  contributions the Dapsone spectrum is rather similar to that of diphenylsulfone discussed earlier.

However, there is one remarkable difference between certain modes of the two molecules. These are normal modes in which the two phenyl rings behave as if they are the strings of two coupled pendula fixed at the sulfone group with a mass at their freely swinging ends, the *para* positions in the rings. The big difference here is that in case of the drug Dapsone the freely swinging mass ( $\text{NH}_2$ ) is about 16 times heavier than the one in diphenylsulfone (H) which – to our knowledge – shows no to only negligible medical activity. These vibrations are low energy ones at  $47$ ,  $147$ , and  $241\text{ cm}^{-1}$  in diphenylsulfone, and at  $32$ ,  $97$ ,  $158$ , and  $365\text{ cm}^{-1}$  for Dapsone. The remarkable difference between the two molecules is that in these normal modes the heavier mass at the ends of the “pendula strings” enforces a much larger out of plane bending than the H atoms can in diphenylsulfone. Likewise, in Dapsone there are two out of plane ring twisting vibrations at  $420$  and  $424\text{ cm}^{-1}$ , which do not occur in the parent diphenylsulfone. Besides the fact that due to the  $\text{NH}_2$  groups the aromatic ring systems in Dapsone should be somewhat more rich in electrons than in the parent, this higher structural flexibility of the phenyl rings in the drug Dapsone than in the non-drug diphenylsulfone could be a hint that this higher flexibility might be a – probably minor (see below) – reason for the drug activity of Dapsone, in that a molecule with more structural flexibility might fit better into receptor sites in cell membranes. This is probably a minor effect for the drug efficiency of Dapsone, since hydrogen bonding should play a far bigger role, while the probably most important fact is the lipophilic nature of Dapsone in contrast to other similar molecules [24],

because *Mycobacterium leprae* contains large amounts of unusual lipids in its cell wall, making it more permeable to Dapsone [24].

## Conclusion

We have made a full assignment of the vibrational spectra of Dapsone and diphenylsulfone to the movements of atoms in the normal modes, using the program GAUSSVIEW. However, a setback of this method is that it does not provide numerical evidence for the assignment. On the other hand, a PED (Potential Energy Distribution) calculation could overestimate the relative importance of certain symmetry coordinates in a normal mode. This is due to the fact that a symmetry coordinate with a relatively large force constant could lead to large PED contributions already at small displacements. Thus we propose that in the future symmetry coordinate calculations should be performed to obtain numerical evidence for the assignment of normal modes to symmetry coordinates. However, this evidence should not be based on PED values but rather on the expansion coefficients of a normal mode in terms of symmetry coordinates, since trustworthy vibrational assignments are very important to identify occurring atomic motions on a quantitative basis on the one hand, and on the other hand to identify reaction mechanisms by carefully monitoring changes in vibrational spectra due to chemical reactions, knowing which atomic motions cause a given vibrational line. For our systems, we have found that the drug Dapsone has a larger structural flexibility in its phenyl rings than the parent compound. This leads to the speculation that this flexibility in the phenyl rings might allow the drug to fit better into receptor sites in cell membranes. However, as detailed above, we assume this structural flexibility to play at best a minor role in the drug activity of Dapsone, if at all. Currently we study a similar molecule as Dapsone, which has hydroxy groups instead of amino groups in the *para* positions of its phenyl rings. Since the mass of an OH group ( $17\text{ amu}$ ) is not much larger than that of an  $\text{NH}_2$  group ( $16\text{ amu}$ ) this molecule should exhibit the same kind of structural flexibility as Dapsone if our speculation is right, because that molecule also shows medical activity. However, again as detailed above, structural flexibility probably plays only a minor role in the drug activity of Dapsone, the most important effects being the lipophilic nature of Dapsone [24] and its ability to form hydrogen bonds.

### Acknowledgements

The authors gratefully acknowledge the support of this work by King Fahd University of Petroleum and Minerals. The authors also greatly appreciate the free ac-

cess to Infrared spectra provided by the National Institute of Advanced Industrial Science and Technology (AIST), Japan through the link <http://www.aist.go.jp/RIODB/SDBS> NO. 7075 and 1420.

- [1] P.M. Wojciechowski, W. Zierkiewicz, D. Michalska, P. Hobza, *J. Chem. Phys.* **2003**, *118*, 10900.
- [2] M. A. Palafox, M. Gill, N. J. Nunez, V. K. Rastogi, L. Mittal, R. Sharma, *Int. J. Quantum Chem.* **2005**, *103*, 394.
- [3] A. K. Rai, S. Kumar, A. Rai, *Vib. Spectrosc.* **2006**, *42*, 397.
- [4] V. Hanninen, L. Halonen, *J. Chem. Phys.* **2007**, *126*, 4309.
- [5] H. M. Badawi, W. Förner, A. A. Al-Saadi, *J. Mol. Struct.* **2004**, *938*, 41.
- [6] M. J. Frisch, G. W. Trucks, H. B. Schlegel, G. E. Scuseria, M. A. Robb, J. R. Cheeseman, J. A. Montgomery, Jr., T. Vreven, K. N. Kudin, J. C. Burant, J. M. Millam, S. S. Iyengar, J. Tomasi, V. Barone, B. Menucci, M. Cossi, G. Scalmani, N. Rega, G. A. Petersson, H. Nakatsuji, M. Hada, M. Ehara, K. Toyota, R. Fukuda, J. Hasegawa, M. Ishida, T. Nakajima, Y. Honda, O. Kitao, H. Nakai, M. Klene, X. Li, J. E. Knox, H. P. Hratchian, J. B. Cross, V. Bakken, C. Adamo, J. Jaramillo, R. Gomperts, R. E. Stratmann, O. Yazyev, A. J. Austin, R. Cammi, C. Pomelli, J. W. Ochterski, P. Y. Ayala, K. Morokuma, G. A. Voth, P. Salvador, J. J. Dannenberg, V. G. Zakrzewski, S. Dapprich, A. D. Daniels, M. C. Strain, O. Farkas, D. K. Malick, A. D. Rabuck, K. Raghavachari, J. B. Foresman, J. V. Ortiz, Q. Cui, A. G. Baboul, S. Clifford, J. Cioslowski, B. B. Stefanov, G. Liu, A. Liashenko, P. Piskorz, I. Komaromi, R. L. Martin, D. J. Fox, T. Keith, M. A. Al-Laham, C. Y. Peng, A. Nanayakkara, M. Challacombe, P. M. W. Gill, B. Johnson, W. Chen, M. W. Wong, C. Gonzalez, J. A. Pople, GAUSSIAN 03 (revision E.01), Gaussian, Inc., Wallingford CT (USA) **2004**.
- [7] F. A. M. Rudolph, A. L. Fuller, A. M. Z. Slawin, M. Bühl, R. A. Aitken, J. D. Woollins, *J. Chem. Crystallogr.* **2010**, *40*, 253.
- [8] R. K. Tiwari, T. P. Singh, *Indian. J. Phys.* **1982**, *56A*, 420.
- [9] W. Förner, W. Utz, *J. Mol. Struct. (Theochem)* **2002**, *618*, 65.
- [10] W. Förner, H. M. Badawi, *J. Mol. Model.* **2001**, *7*, 288.
- [11] G. W. Chantry in *The Raman Effect*, Vol. 1, (Ed.: A. Anderson), Mercel Dekker, New York **1971**, chapter 2.
- [12] C. Rios, J. Nader-Kawachi, A. J. Rodriguez-Payan, C. Nava-Ruiz, *Brain Res.* **2004**, *99*, 212.
- [13] D. Sangiolo, B. Storer, R. Nash, L. Corey, C. Davis, M. Flowers, R. C. Hackman, M. Boeckh, *Bio. Blood and Marrow Transplant.* **2005**, *11*, 521.
- [14] E. N. Alves-Rodrigues, L. C. Ribeiro, M. D. Silva, A. Takiuchi, O. C. Rabel-Filho, D. Martini-Filho, C. J. F. Fontes, *Amer. J. Kidney Diseases* **2005**, *46*, 51.
- [15] P. Bhaiya, S. Roylchowdhury, P. M. Vyas, M. A. Doll, D. W. Hein, C. K. Svensson, *Toxicology and Applied Pharmacology* **2006**, *215*, 158.
- [16] J. Fukae, K. Noda, K. Fujishima, R. Wada, T. Yoshiike, N. Hattori, Y. Okuma, *Clinical Neurology and Neurosurgery* **2007**, *109*, 910.
- [17] P. M. Naik, G. M. Lyon III, A. Ramirez, E. C. Lawrence, D. C. Neujahr, S. Force, A. Pelaez, *J. Heart and Lung Transplant.* **2008**, *27*, 1198.
- [18] W. Billard, H. Binch III, K. Bratzler, L. Chen, G. Crosby, Jr., R. A. Duffy, S. Dugar, J. Lachowicz, R. McQuade, P. Pushpavanam, V. B. Ruperto, L. A. Taylor, J. W. Clader, *Biorg. Medicinal Chem. Lett.* **2000**, *10*, 2209.
- [19] G. L. Almajan, S. Barbuceanu, E. Almajan, C. Draghici, G. Saramet, *Europ. J. Medicinal Chem.* **2009**, *44*, 3083.
- [20] R. D'Cunha, V. B. Kartha, S. Gurnani, *Spectrochim. Acta* **1983**, *39A*, 331.
- [21] Infrared spectra of the molecules (Nujol mull): [aist.go.jp/RIODB/SDBS](http://aist.go.jp/RIODB/SDBS) NO. 7075 and 1420.
- [22] Raman spectra of the molecules (solids and in solution): [sigmaaldrich.com](http://sigmaaldrich.com).
- [23] W. Förner, *Intern. J. Quant. Chem.* **2004**, *99*, 533.
- [24] T. Scior, G. Raddatz, R. Figueroa, H. J. Roth, H. A. Biswanger, *J. Mol. Model.* **1997**, *3*, 332.